



Probing the Ionosphere with the Very Large Array

Rick Perley (NRAO)
Gary Bust (ARL, U.TX)





Resolution in Astronomy



- In radio astronomy, angular resolution is generally limited by diffraction:

$$\theta \sim \lambda/D.$$

- Modern astronomy requires at least 1'' resolution, for which the corresponding physical aperture must be:

$$D > 2 \times 10^5 \lambda$$

- The only means of obtaining such effective apertures at radio wavelengths is through interferometers, using the well-established technique of 'aperture synthesis'.



Fourier Synthesis



- The use of radio interferometers for imaging in astronomy relies on a fundamental theorem in optics (the Van Cittert-Zernicke theorem):
 - The Spatial Coherence Function is the Fourier transform of the Sky Brightness:

$$V(u, v) \Leftrightarrow I(l, m)$$

where: $V(u, v)$ is the spatial coherence function ('Visibility')

$I(l, m)$ is the sky brightness

and: (u, v) are the spatial baseline coordinates (wavelengths)

(l, m) are the angular coordinates (direction cosines)

- The visibilities $V(u, v)$ are measured by phase-coherent interferometers.



Phase-Stable Interferometers



- However, the measures of the visibility that are obtained are not those we desire -- they have been corrupted by various disturbing influences.
- The measured quantity, $V_m(u,v)$ is related to the true visibility by:

$$V_m(u, v) = g_i g_j^* V(u, v)$$

where:

$$g_i = a_i e^{i\phi_i}$$

is the complex gain for antenna 'i'.

- There are many contributors to the complex gain -- for our purpose, we consider only that due to perturbations caused by fluctuations in the propagation path.



Astronomical Calibration



- Calibration of the visibility data requires measurement and removal of the instrumental and atmospheric contributions to the gain.
- Over the past 20 years, astronomers have developed powerful algorithms to permit removal of the gain.
- These are based on a LSQ solution for the N gain terms from the $\sim N^2/2$ visibility measures obtained from observations of a source with known structure.
- For astronomers, these gain terms are a nuisance, to be thrown away once their effects are corrected for.
- However, these discarded gains include information on atmospheric phenomena, and may be of some use...



Ionospheric Effects



- The effects of the ionosphere upon radio propagation are well known.
- For our frequencies, the change in refractive index is:

$$\Delta\mu = 1 - \mu \approx 40.5N / \nu^2$$

where N = electron density (m^{-3}), and ν = frequency (Hz)

- Integrated along a propagation ray, the change in phase-path is:

$$\Delta L = -\int_0^s \Delta\mu dl = -0.405 \frac{N_{TU}}{\nu_G^2} \text{ meters}$$

where N_{TU} is the column density in units of 10^{16} electrons/ m^2 , and ν_G is the frequency in GHz.



Ionospheric Phase



- Converted into terms of phase,

$$\Delta\phi = 2\pi\Delta L / \lambda = -8.48 \frac{N_{TU}}{\nu_G^2} \text{ radians}$$

where

N_{TU} = column density in units of 10^{16} electrons/m²

ν_G = frequency in GHz



Typical Ionospheric Perturbations



Typical values of ionospheric perturbations are given below for a column density of 10 TU units = 10^{17} electrons/m².

Characteristic	Typical Value (at 100 MHz)	Frequency Scaling
Phase-path Length	-400 meters	ν^{-2}
Phase Change	-840 radians	ν^{-1}
Refraction	1.3 arcminutes	ν^{-2}
Polarization Rotation	6.6 radians*	ν^{-2}
Attenuation	0.01 dB	ν^{-2}

* Note for radio astronomers -- this is an RM of only 0.7 rad/m².



Interferometer Phase



- However, an interferometer is not sensitive to this total phase path perturbation, but rather is sensitive to the difference:

$$\delta\phi = -8.48 \delta N_{TU} / \nu_G \text{ radians}$$

- Where δN_{TEC} is the difference in the column densities, in TUs, between the two paths.
- Note that an interferometer cannot detect the phase change induced by a plane-parallel atmosphere.
- But it is very sensitive to deviations from a plane-parallel geometry, caused e.g. by atmospheric fluctuations, or earth curvature.



Phase Stability



- A modern interferometer can have a phase stability of better than one electrical degree over timescales of hours.
- At this level of stability, an interferometer can detect a column path change (in TUs) of:

$$\delta N_{TU} \sim 2 \times 10^{-3} \nu_G$$

- Thus at a frequency of 100 MHz, a change in TEC of 0.02% of one TEC unit can be detected.
- Even in a more practical case, where the phase stability is ~ 10 degrees, a perturbation of 0.2% of a TEC unit ($\sim 10^{13}$ electrons/m²) can be easily detected.



The Very Large Array



- The Very Large Array (VLA) is the world's premier radio synthesis interferometer.
- The array comprises 27 movable antennas on three arms.
- Four configurations – 1 to 35 km. max. baseline
- Correlator products from all 351 baseline combinations are formed.
- The array is outfitted at 8 frequency bands, including 327 and 73.8 MHz, where ionospheric perturbations dominate the phase stability.



VLA Layout

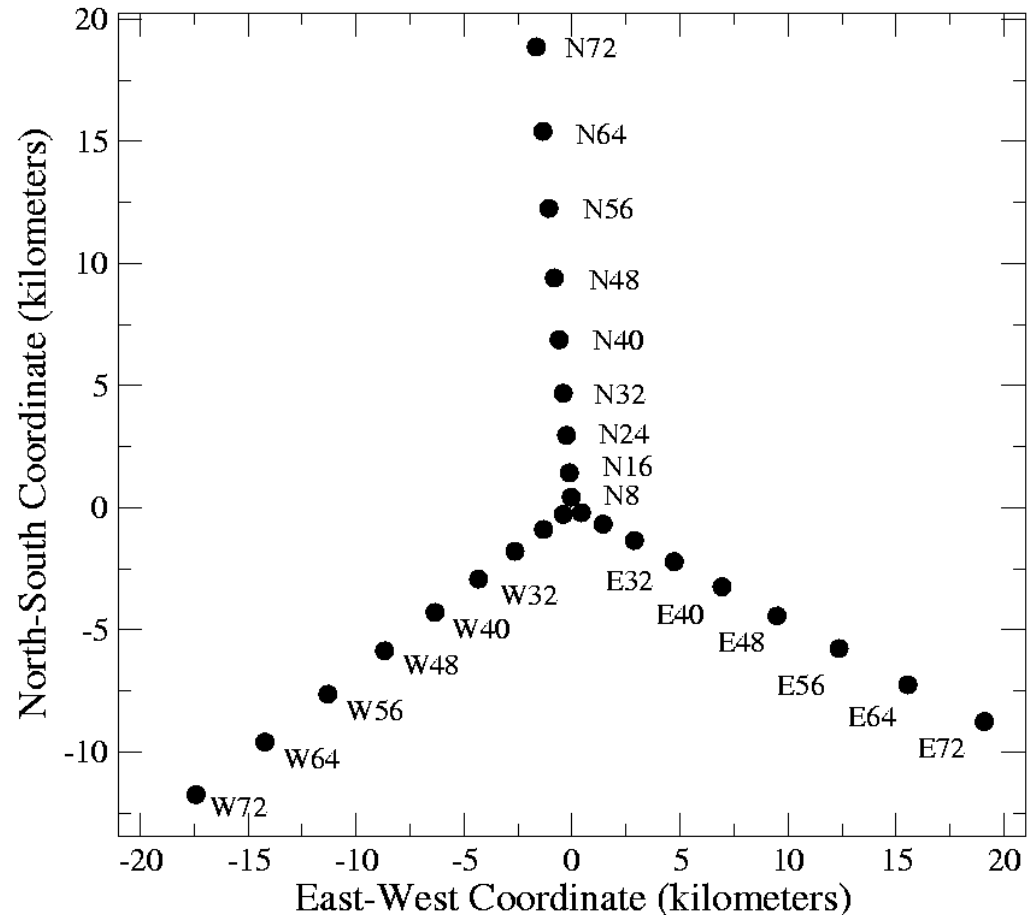


- The VLA comprises 27 antennas, with 9 on each of three arms.

- In its largest ‘A’ configuration, the arms extend ~20 km from the array center.

- Array long. = 107.6
- Array lat. = 34.1 N
- Located in central New Mexico.

The Very Large Array
Array Layout (A-Configuration)





VLA Typical Observing



- The VLA has two frequency bands, centered near 327 and 73.8 MHz where the gain phase stability is clearly dominated by ionospheric fluctuations.
- Various phenomena are repeatedly seen in the astronomical data – TIDs, large-scale wedges, various small-scale phenomena, and occasionally scintillation.
- Because most observations are broken into disconnected short ‘glimpses’, it is difficult to comprehensively classify (or study?) ionospheric phenomena in these data.
- Occasionally, a single long observation is undertaken -- the following examples come from a 12-hour observation at 73.8 MHz of the prominent radio source Virgo A, on the night/morning of 19 January, 2001.

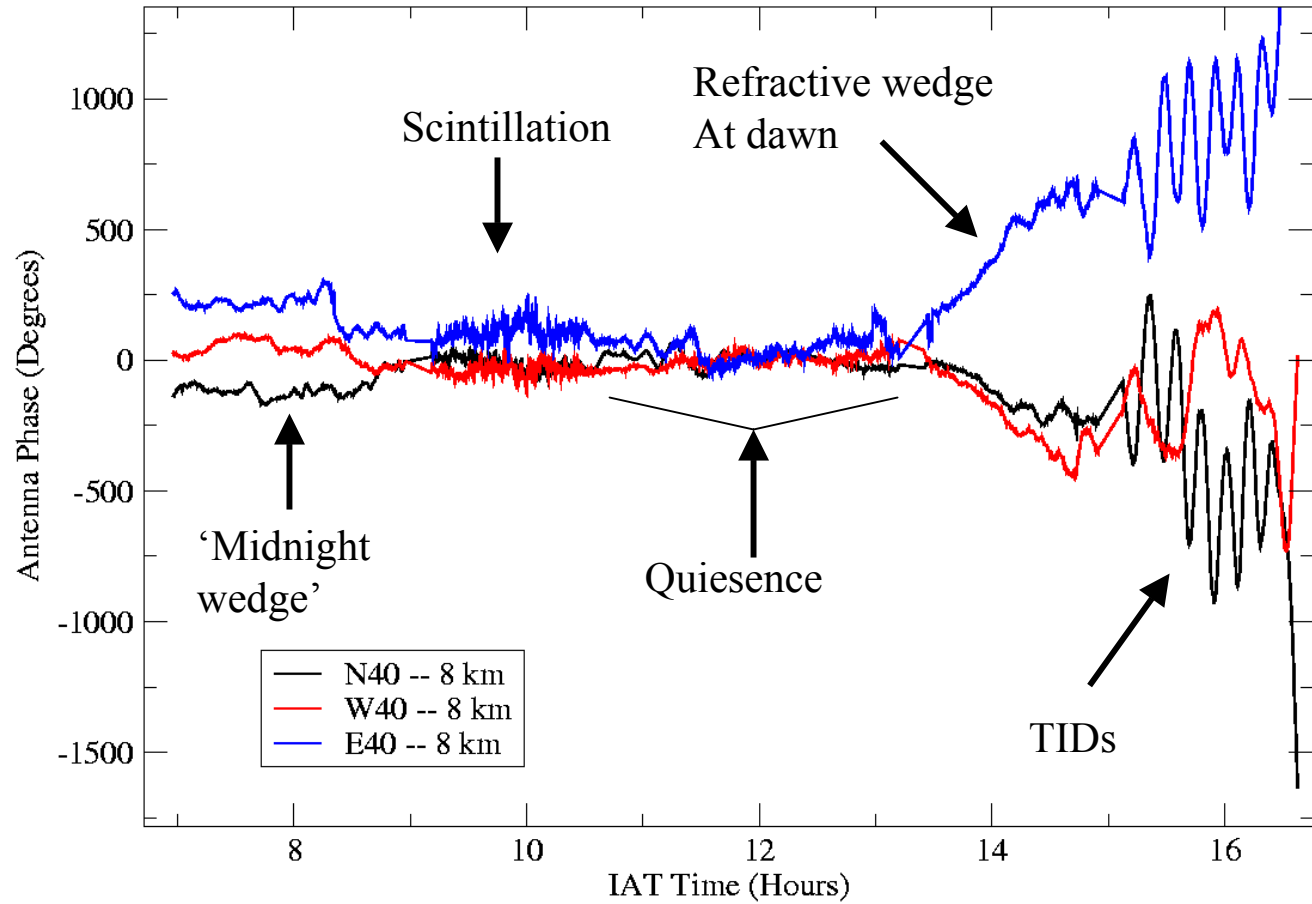


Antenna Phase on 3 Arms



The phase on three 8-km spacings at 3 different azimuths.

A wide range of phenomena were observed over the 12-hour observation.

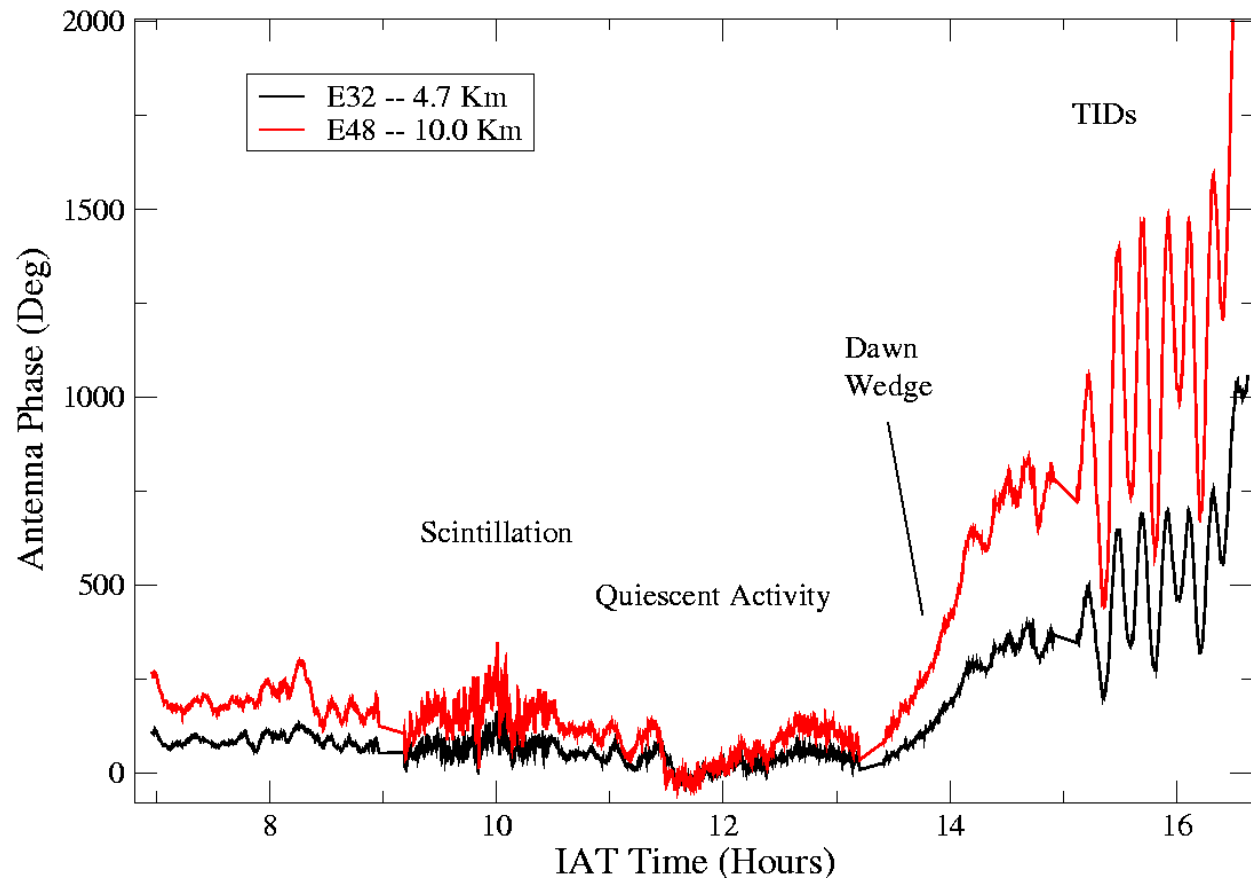




Phase proportional to baseline



- Two antennas, at different distance, along the same azimuth. The phase appears proportional to baseline length.

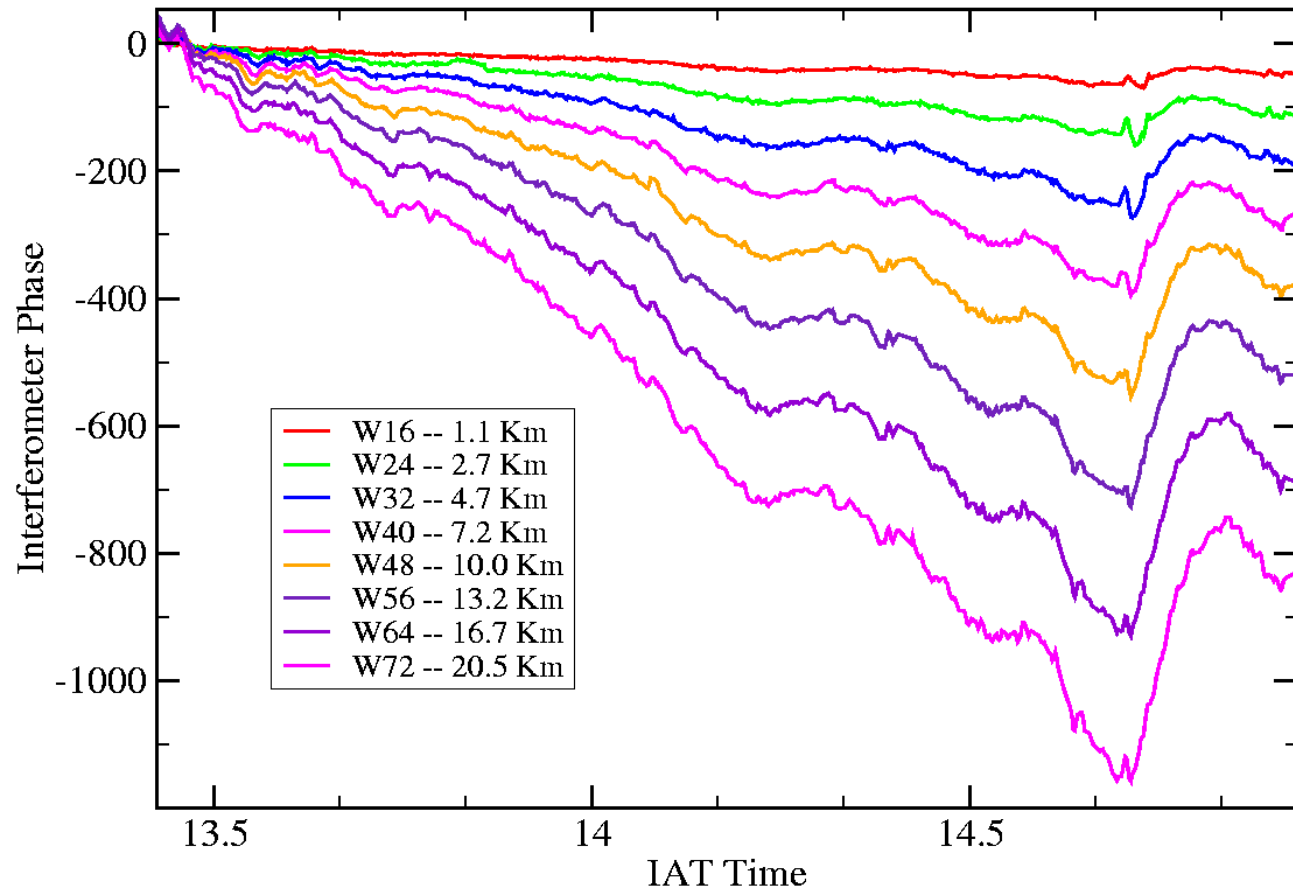




Dawn Wedge Phase



All antennas on West Arm during 'Dawn Wedge' period.



This shows a thickening wedge over the array which started about 1 hour before dawn, and was terminated by the onset of a large wave event.

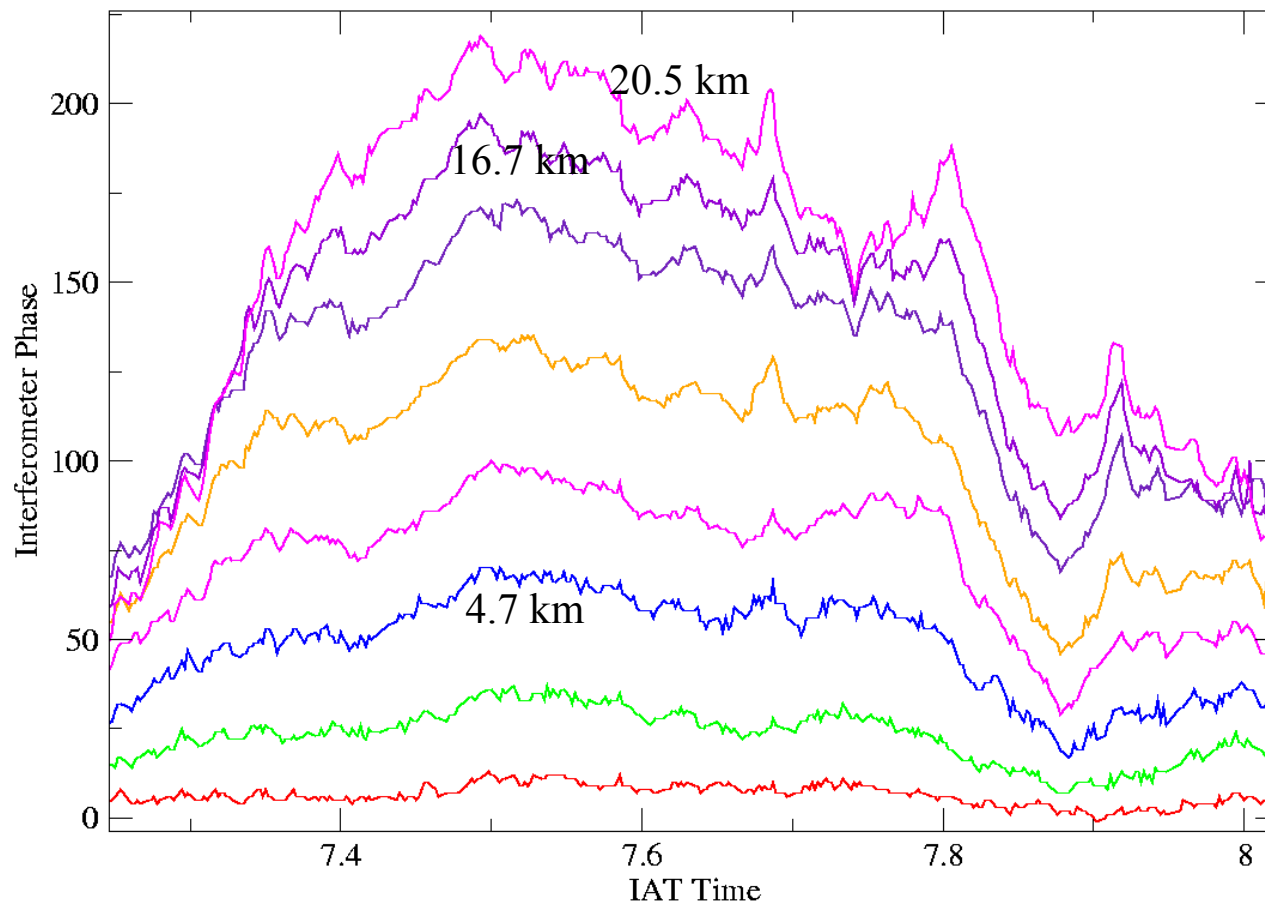


Non-linear phase in midnight wedge



- In this example, the phases are not strictly proportional to baseline length -- there is significant curvature in the wedge.

The phase gradient is much steeper in the inner part of the arm than on the outer part.



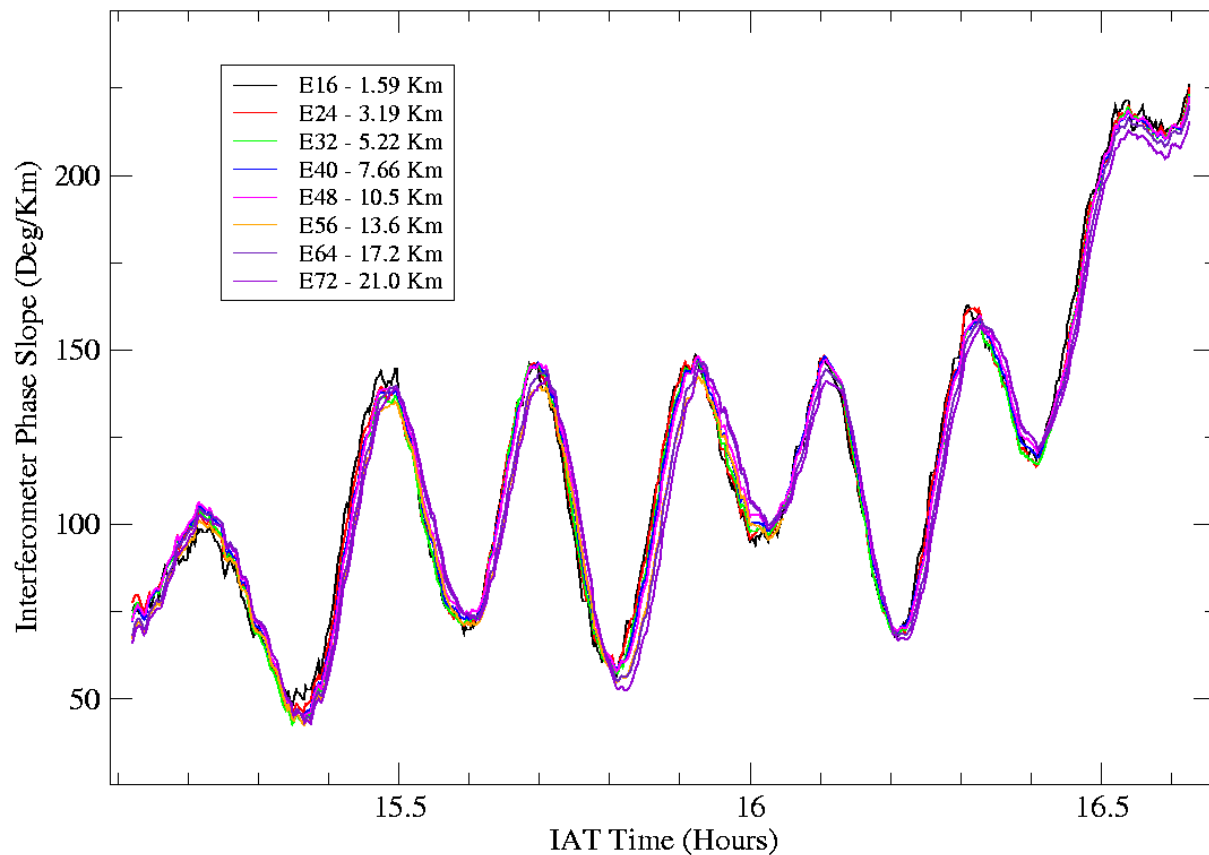


East Arm Phase Gradient



During the period of large-scale waves, the phase gradient is remarkably uniform down the entire arm.

Careful inspection shows a small time lag between the outer and inner antennas.



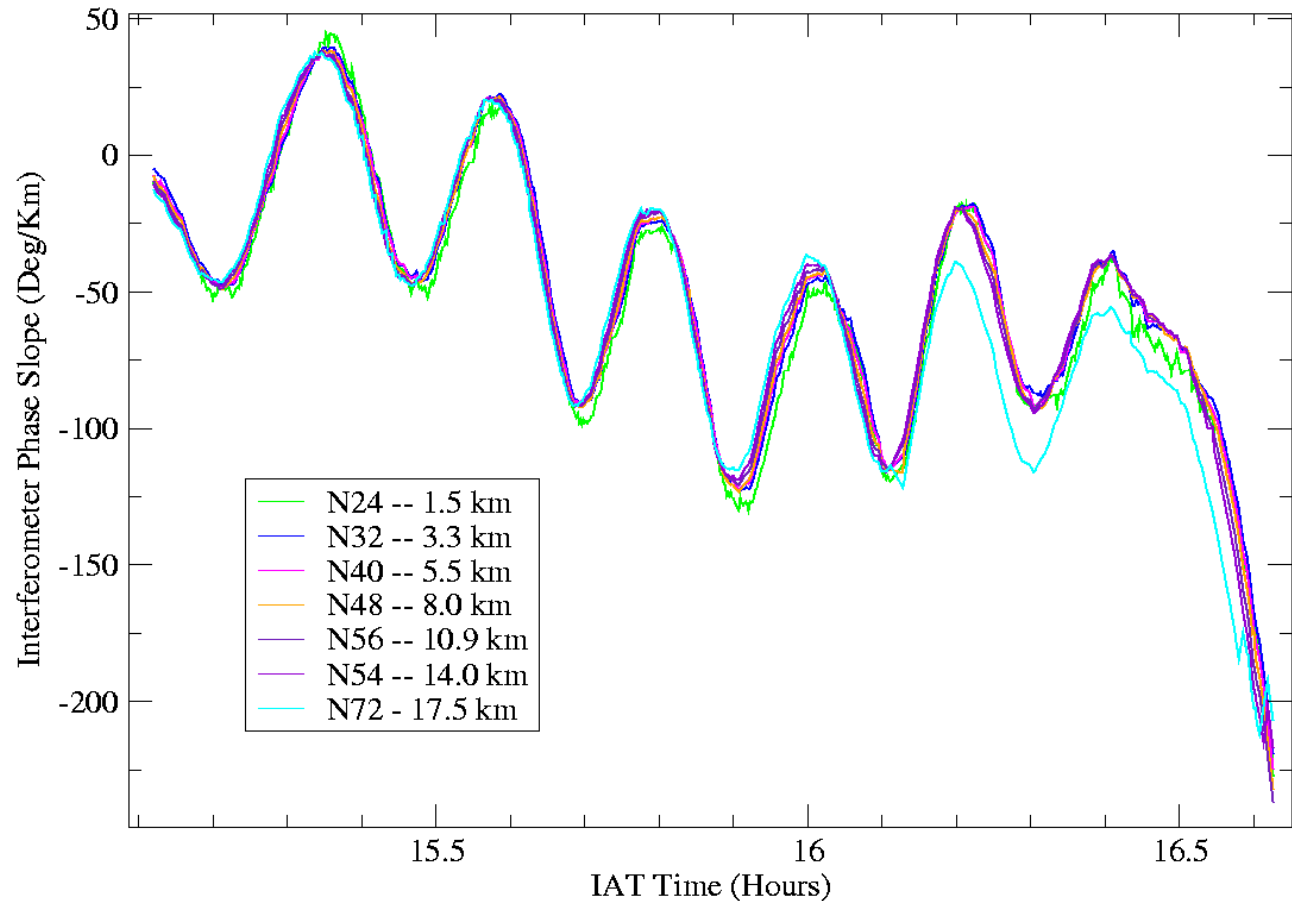


North Arm Phase Gradient



- The same plot, for the north arm antennas.

Again, a small time lag is seen between the inner and outer antennas.



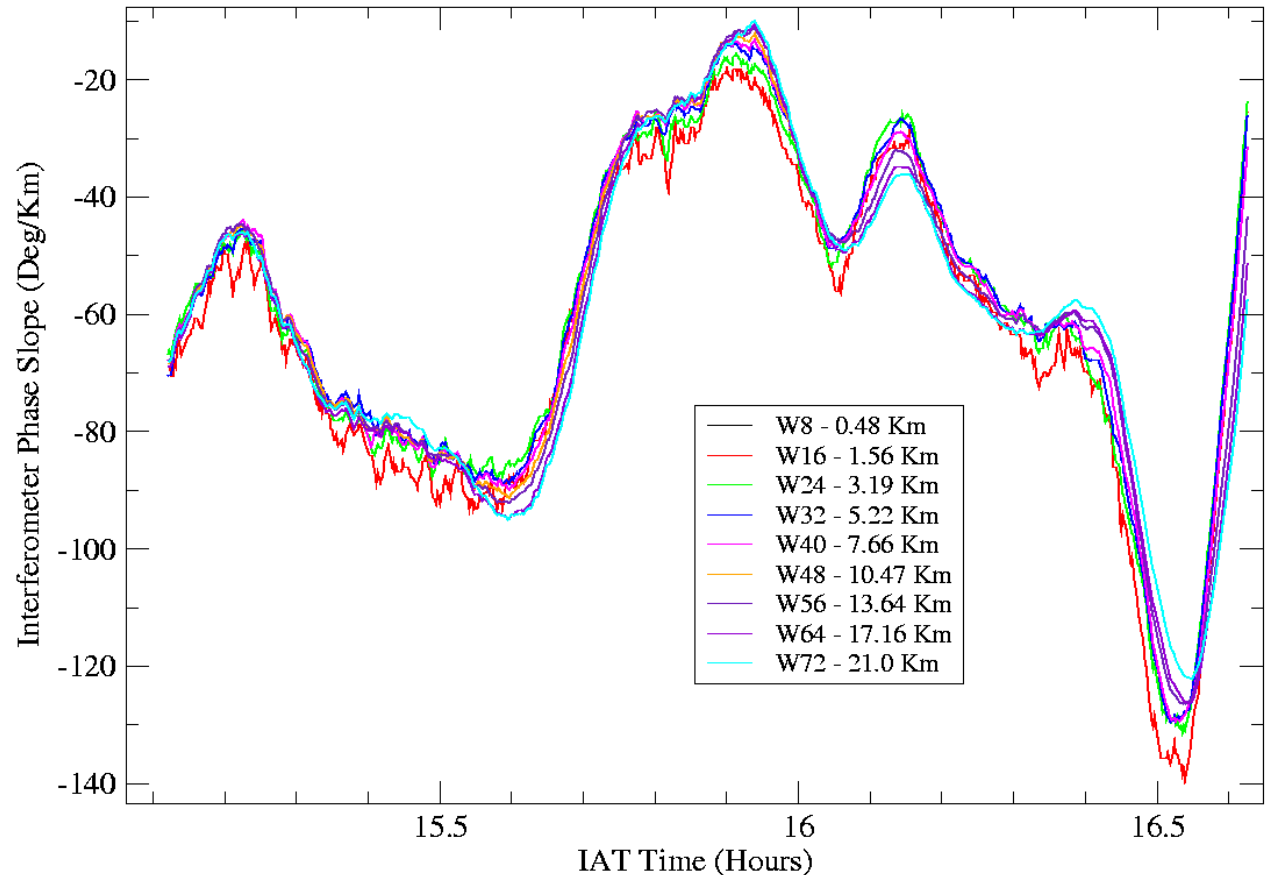


West Arm Phase Gradient



The scaling for the west arm is as good, but the pattern is different

The simplest explanation is that the waves are moving orthogonally to the SW arm.





Traveling Wave Model



- The organized wave pattern, and its scaling and similarity along each arm argues for a long-wavelength, high velocity wave motion in the ionosphere.

- Writing
$$\phi = A \cos(kx - \omega t)$$

$$k = 2\pi / \lambda$$

$$\omega = 2\pi v / \lambda$$

where λ = wavelength, and v = wave velocity.

- The interferometer phase can be found to be

$$\phi_{ij} = 2A \sin(kB / 2) \sin[\omega t - k(x_i + x_j) / 2]$$

where $B = x_i - x_j$ = baseline length.



Model applied to the TIDs



- This formalism can be easily fit to the period of travelling waves. The observed values are:
 - $T = \text{period} \sim 750 \text{ sec}$
 - $S = \text{phase slope} \sim 50 \text{ deg/km}$
 - $\delta t = \text{time lag} \sim 50 \text{ sec over } 20 \text{ km.}$
- From these, we can derive the following:
 - $V = 200 \text{ m/sec}$
 - $\lambda = 750 \text{ km}$
 - $A \sim 130 \text{ radians}$
- The wave amplitude is $\delta N_{\text{TEC}} \sim 1.1 \text{ TUs.}$
- The direction is NW to SE (approximately).

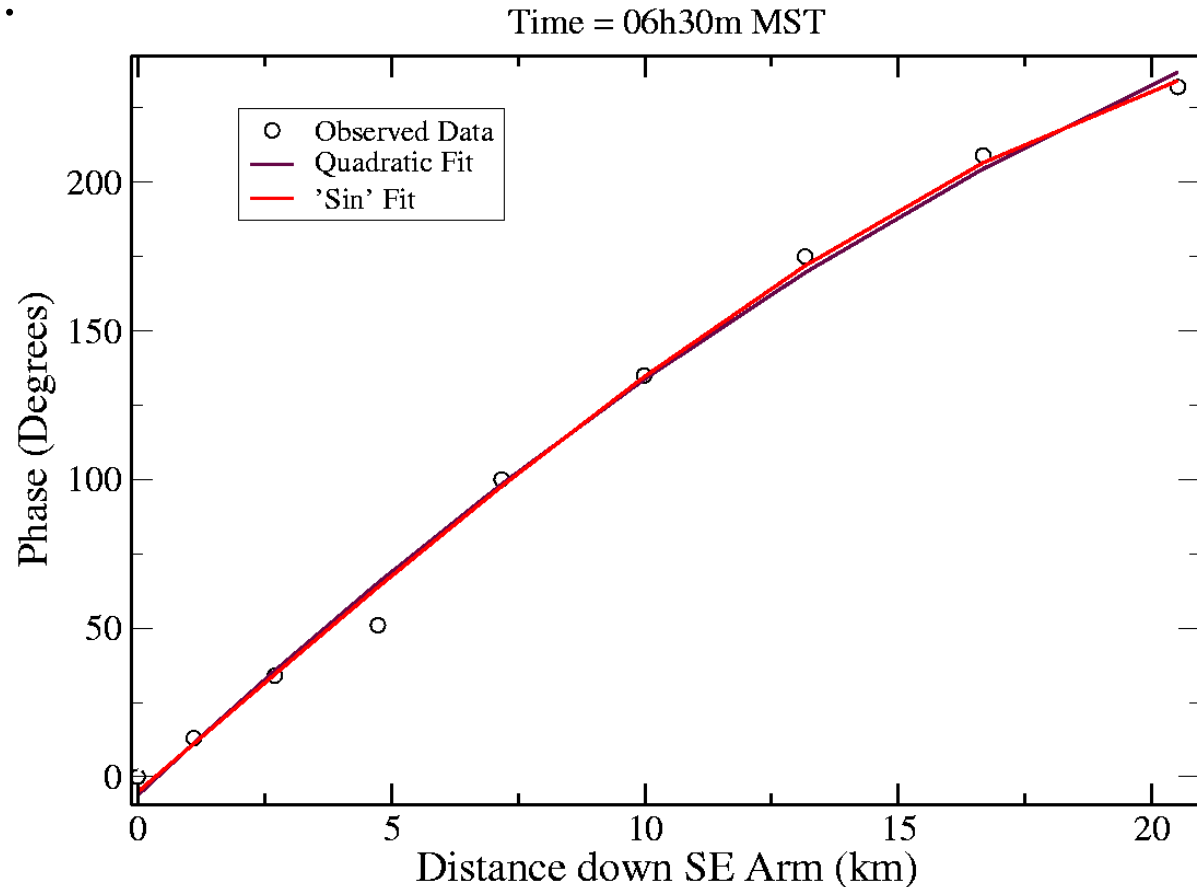


Non-Linear Phase Screen



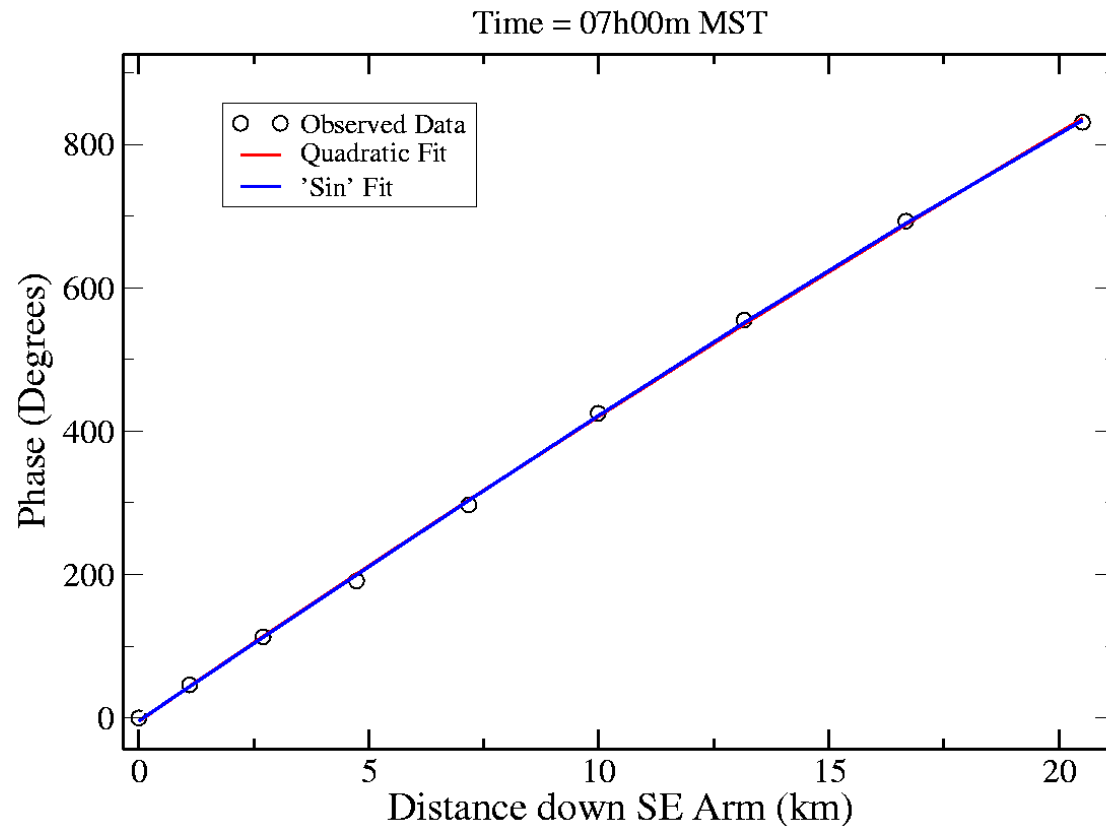
- During the 'dawn wedge', the phase screen is non-linear.

This fit is for early times, when the wedge was just visible.



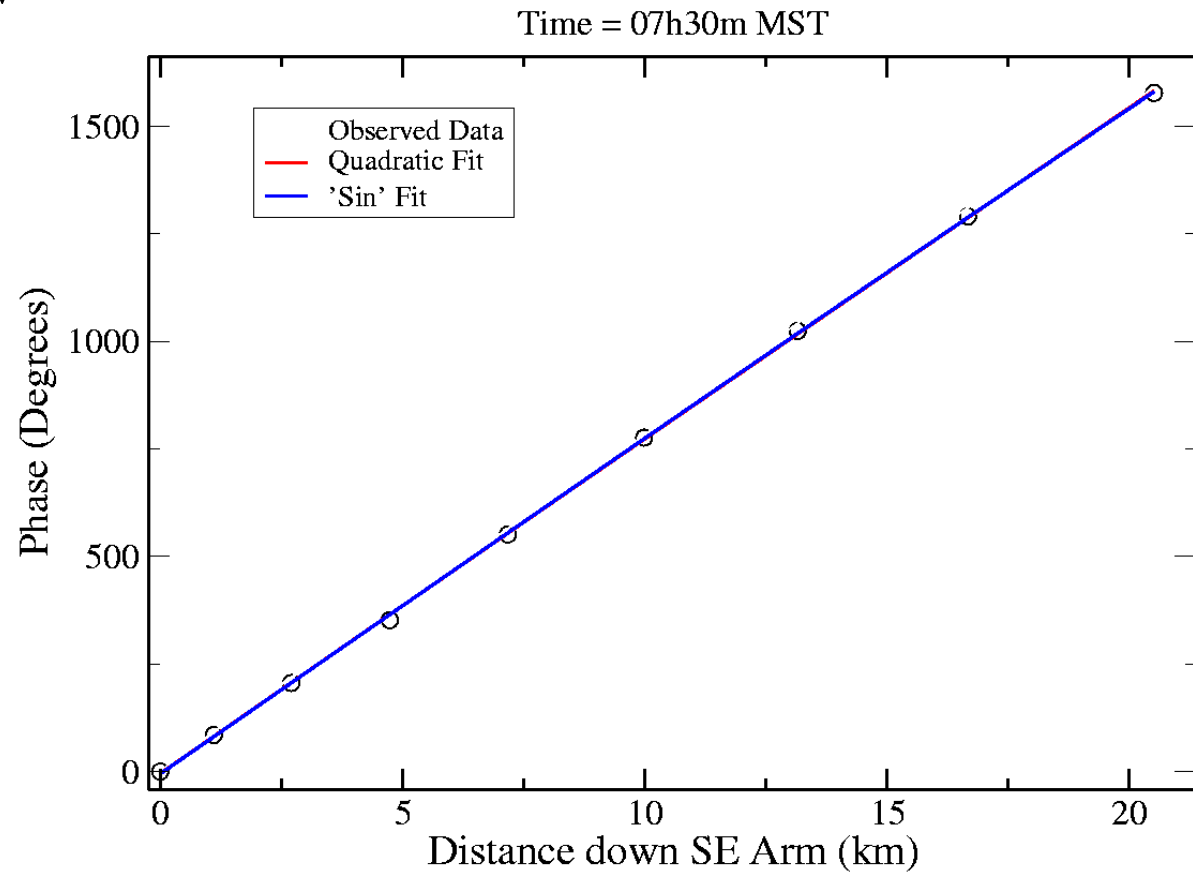


- A half hour later – gradient is higher, and the curvature less.





- As the sun rises, the gradient is maximum, but the curvature is very small



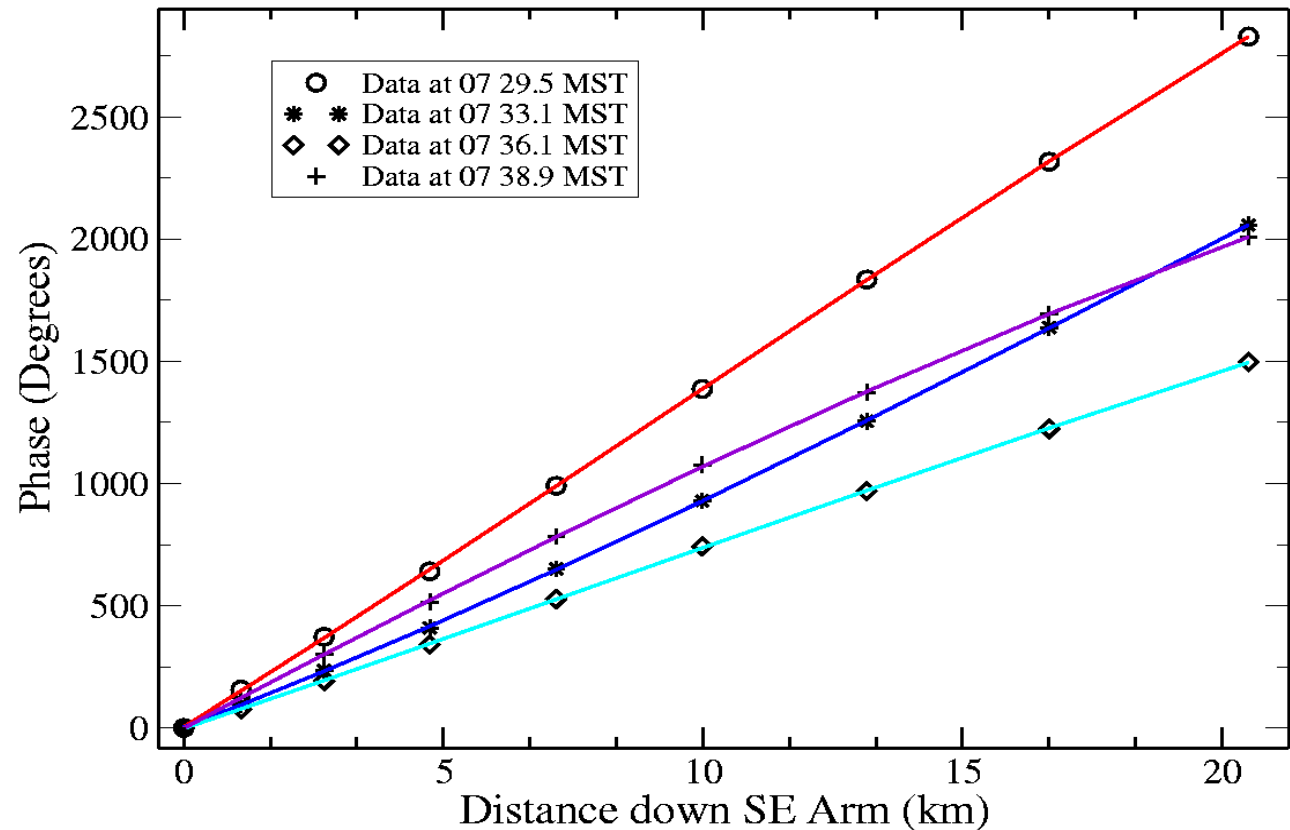


TID Curvature



- The curvature is easily seen during the traveling TIDs.

The amplitude and sign of the curvature fits a wavelength of 750 km with amplitude of 130 radians.





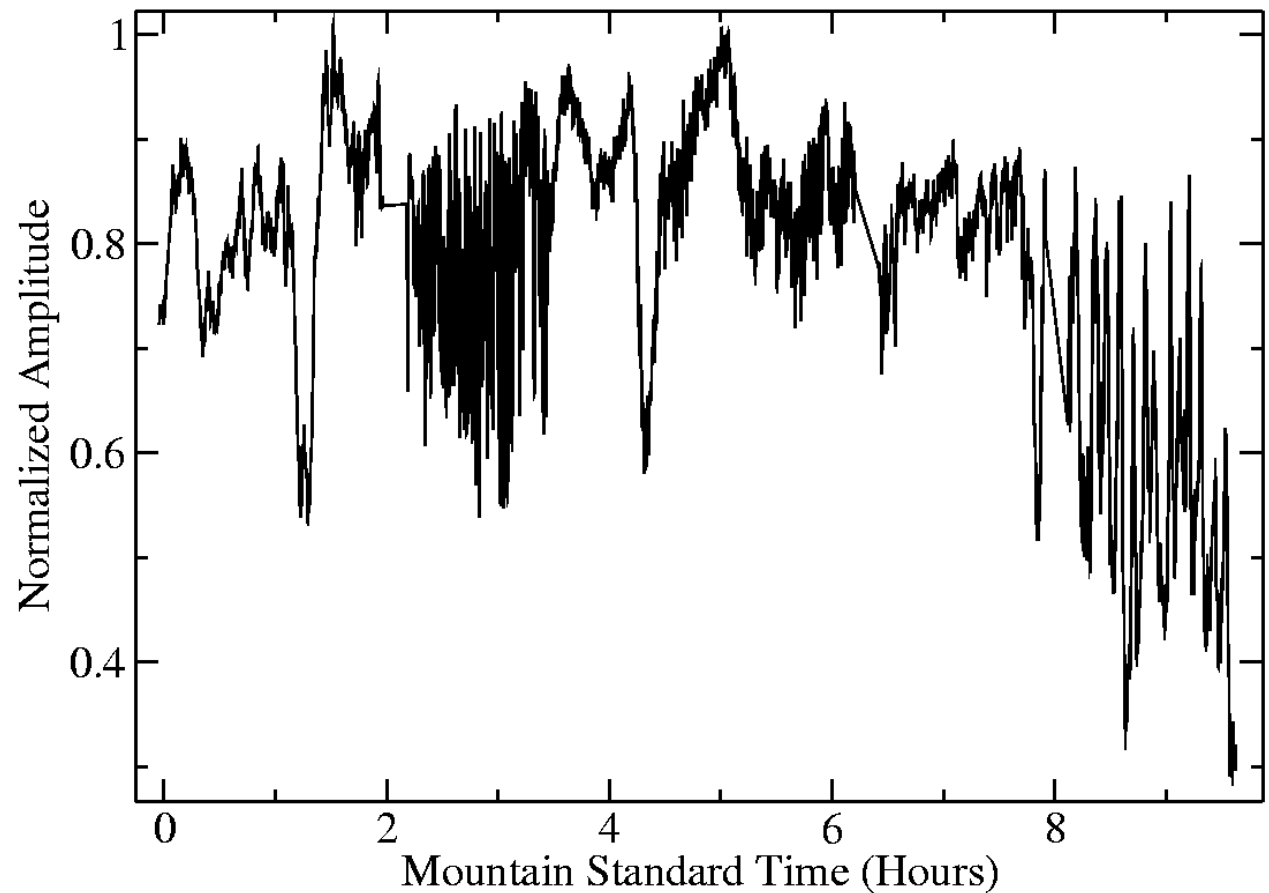
- So although the wavelengths can be very long, and the curvature in the front appear small, this curvature remains significant, and will cause distorting effects in the astronomical image.
- This effect is most easily seen in the image plane.
- Instantaneous observations ('snapshots') can be made to track the refractive motion (due to the gradient) and distortions (from higher order terms) due to the screen.
- The results are highly instructive ...



Defocusing of Virgo A



- The instantaneous amplitude of the radio source





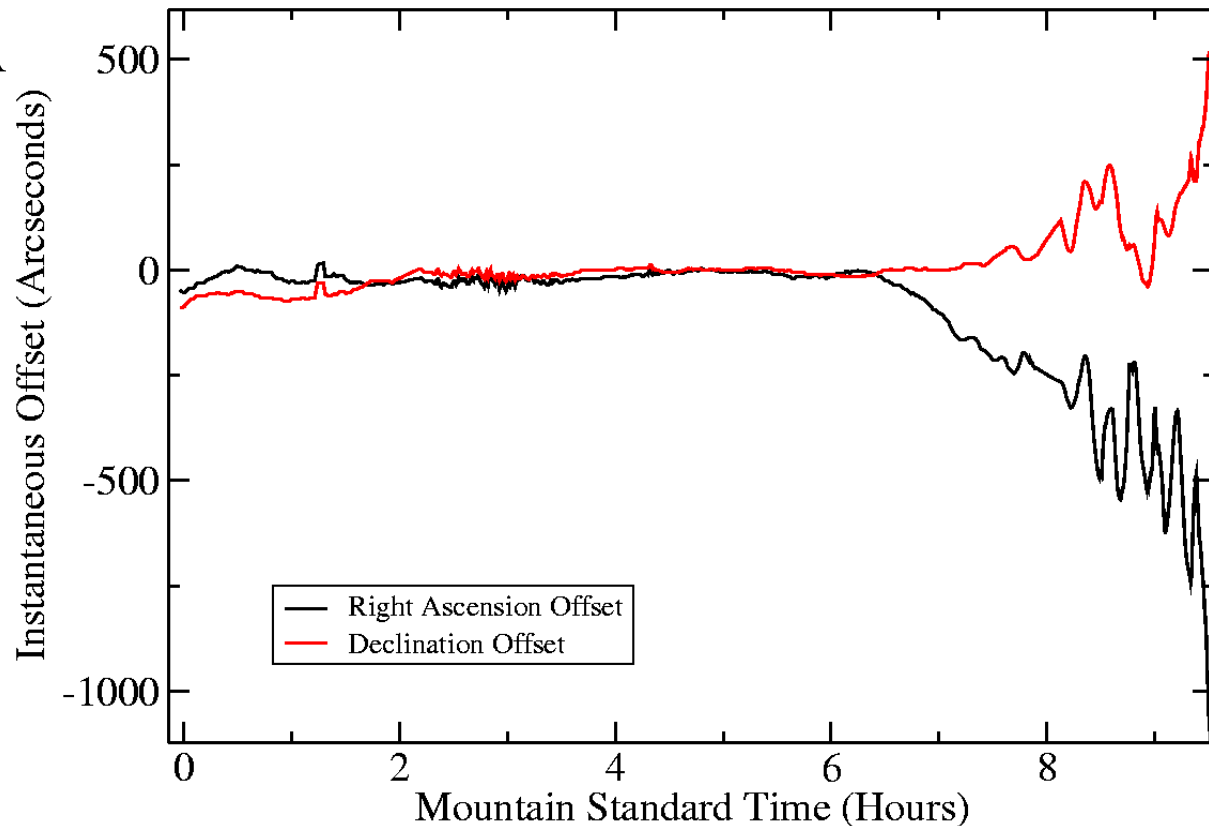
Refraction of Virgo A



- Apparent Position of Virgo A Radio Source

A west offset in RA
is positive.

A north offset in
is positive.





- The instantaneous positions show:
 - Slow relative motions during the quiescent periods
 - Small, rapid oscillatory motion during the ‘scintillation’ period
 - Very large and relatively slow oscillatory motion during the large TID period.



Differential Offset



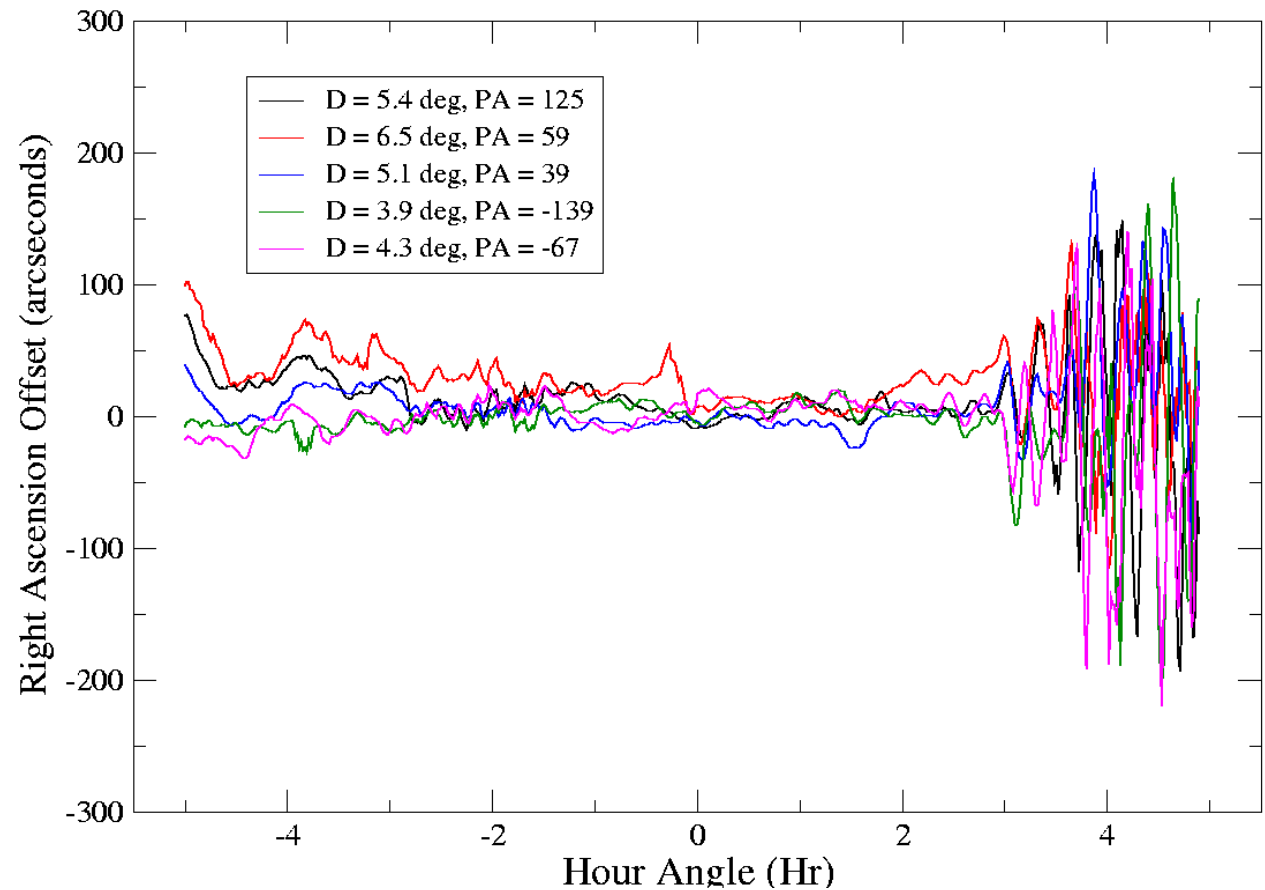
- These large ionospheric perturbations can be removed from the data, and images of other, nearby objects can be made, to observe their differential motions.
- The simple wave model shown predicts 1 radian phase differentials on angular scales of ~ 1 degree, during the TID period.
- This will cause easily detected differential motions in such objects.
- There are ~ 5 objects within 6 degrees of the Virgo A radio source which can be detected, and tracked, in observations short enough to allow motion tracking.



Virgo A differential motions



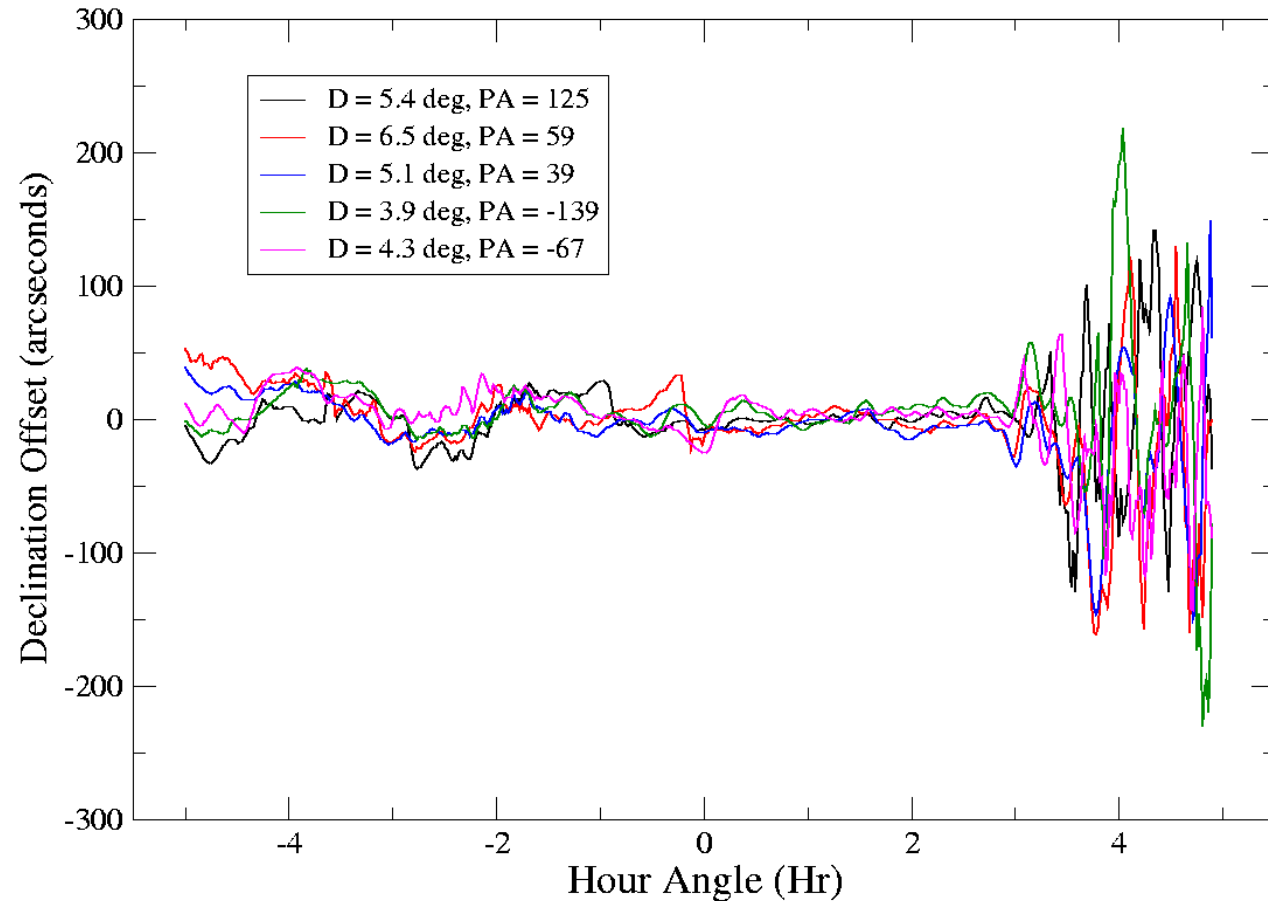
- The differential offsets in Right Ascension



Declination differentials



- The differential offsets in Declination





Tomography with the VLA?



- The presence of so many detectable objects within each antenna's beam suggests a 3-d mapping of the screen may be possible.
- Each antenna beam 'illuminates' about 80 km of the ionosphere -- much larger than the array.
- There is a ~ 55 km region seen by **all** antennas, each with a different line of sight.
- This should permit 3-dimensional discrimination of phase perturbations, with resolution $\sim 50 \times 50 \times 250$ meters, with accuracy of $\sim .001$ TU.



Summary



- Astronomers have built large, phase-coherent arrays.
- They plan to build much bigger ones!
- These instruments are very susceptible to ionospheric perturbations on all scales.
- Astronomers have developed or are developing powerful methods to remove these perturbations.
- They then throw away these data!
- Perhaps there is some gold amongst this refuse?